Acoustic disruption of tumor endothelium and on-demand drug delivery for cancer chemotherapy

Junhua Xu,[a,c] Honglei Tu,[b,a,c] Zheng Ao,[a] Yifan Chen,[a] Ryan Danehy,[a] and Feng Guo[a,*]

[a.] Department of Intelligent Systems Engineering, Indiana University, Bloomington, Indiana 47405, United States

[b.] Department of Hematology, Zhongnan Hospital of Wuhan University, Wuhan, Hubei 430072, China

[c.] Contribute equally to this work

*E-mail: fengguo@iu.edu

Abstract: Chemotherapy has been the most widely used treatment against cancer, however, is limited by its systemic toxicity as well as its resistance developed by tumors' physical barriers. Herein, we propose a novel acoustically-mediated treatment regime to on-demand release therapeutics and disrupt tumor structures. By programming a high intensity focused ultrasound (HIFU) transducer, we can locally and digitally release gemcitabine (GEM) as well as open a local blood-tumor barrier or even tumor stroma to enhance intratumor drug delivery via acoustically-oscillating bubbles and liposomes. In our experiments, we modeled tumor endothelium by culturing a monolayer of murine endothelial cells (2H11) on transwell membrane. We locally disrupted the cultured endothelium to enhance drug penetration by using perfluorocarbon (PFC) liquid droplets as breaking probes and protoporphyrin IX (PPIX) hybridized liposomes as drug carriers. We also demonstrated an on-demand release of GEM by digitally triggering the break of drug carriers. Moreover, we validated the acoustic tumor endothelium disruption in vivo by monitoring penetration of dye (Evans blue) in solid tumors. Therefore, we present an acoustically-mediated delivery method that both releases drug on-demand locally and opens the blood-tumor barrier to enhance drug penetration. This sets the ground for further clinical cancer therapy to improve many systemic cancer treatments.

Key Words: Drug Delivery, Cancer Treatment, Tumor Endothelium, HIFU

1. Introduction

Pancreatic cancer accounts for 3% of cancers across the United States, yet it yields one of the worst prognosis with the lowest overall survival rate among the most common cancers[1][2]. The American Cancer Society predicts that there would be 55,440 new cases and 44,330 death cases of pancreatic cancer in the United States in 2018[3]. The overall 5-year survival rate of pancreatic ductal adenocarcinoma (PDAC), a major type of pancreatic cancer, is only about 6%[3]. Chemotherapy is one of the primary cancer treatments for pancreatic cancer. However, chemotherapeutic drugs for pancreatic cancer are not tumor specific and frequently bring significant and systemic toxic effects to non-cancerous tissues. On the other hand, pancreatic cancer cells develop resistance to chemotherapy by biological mutations and physical barrier, and the latter is mostly due to dense tumor stroma and lack of abundant vessels. Among clinical chemotherapeutics, gemcitabine (GEM) is one of the most effective drugs in treating pancreatic cancer as well as other solid tumors (bladder, breast, ovarian, thyroid, and multiple myelomas)[2][4]. However, current systemic GEM administration reduces the drug effectiveness due to the short plasma half-life, insufficient intratumor diffusion, drug resistance, and systemic toxicity[5][6]. Moreover, GEM has to be administered systemically and repeatedly in clinical practices in order to maintain an effective therapeutic concentration [5], which worsens the side effects. Thus, to improve chemotherapy specificity and efficiency, a method to locally deliver treatment agents, enhance local penetration, and better control of drug delivery dynamics is highly desired.

To meet these needs, a variety of drug delivery strategies have been developed to encapsulate or mix anticancer drugs into delivery vesicles and smartly release these carried drugs into tumor microenvironments. Recently, polymeric nanoparticles[7], micelles[8], liposomes[9], and polymer-drug conjugate[10] have been widely explored as drug carriers. Meanwhile, a variety of trigger mechanisms such as pH[8], enzyme digestion [11], redox potential[12], temperature[13], and light[14], have also been experimented to selectively or actively release the chemotherapeutics from their carriers into the tumor. Among many delivery methods, acoustically-mediated delivery has been an alternative solution by noninvasively shooting highly intensive focused ultrasound (HIFU) to acoustically-responsive vesicles for local drug release. Compared to light-triggered drug delivery[15], acoustically-mediated delivery can provide a better penetration depth yet a reasonable spatial precision to deliver the chemotherapy treatment locally for patients[16]. In addition, during the acoustically-mediated delivery, acoustically-oscillating bubbles are used to noninvasively break the blood-brain barrier (BBB) [17]. Similarly, acoustic droplet vaporization has been employed to disrupt vessels in tumors directly [18]. One problem of HIFU treatment is that the HIFU may have genotoxicity because DNA damage of cells has been observed after the HIFU exposure[19][20]. The other problem is that the HIFU is

strongly attenuated by bone[21]. A recent clinical application of magnetic resonance imaging (MRI) system may correct the attenuation and make it possible to deliver therapeutics across the brain skull[22]. However, simultaneous localized delivery and opening of blood-tumor barrier upon single acoustic treatment has not been demonstrated yet.

Herein, we propose a novel method to improve cancer chemotherapy efficiency utilizing HIFU (Fig.1). We can achieve both on-demand drug release and enhancement of drug penetration through tumor endothelium simultaneously by co-delivery of microbubbles and liposome vesicles. Under acoustic treatment, liquid PFC droplets are vaporized into microbubbles, and these microbubbles oscillate at high frequency. These acoustically-oscillating microbubbles can enhance chemotherapy effectiveness by disrupting the tumor endothelial barrier via creating pores and/or intracellular gaps to endothelium. Meanwhile, the liposomes hybridized with the sonosensitizer (PPIX) could be broken down for on-demand drug release by programmed HIFU insonation[23]. The proposed approach could release drugs or therapeutics on-demand as well as enhancing penetration of blood-tumor barrier in a digital and repetitive manner, leading to an enhanced antitumor therapeutic effect.

2. Experiment

2.1 Materials and cell lines. 1,2-distearoyl-sn-glycero-3-phosphatidylglycerol (DSPG),1,2-dilinoleoyl-sn-glycero-3 phosphocholine (DLPC), 1,2-distearoyl-sn-glycero-3-phosphocholine (DSPC) and cholesterol were purchased from Avanti Polar Lipids. 6-carboxy-2',7'-dichlorodihydrofluorescein diacetate (Carboxy-H2DCFDA) was purchased from Thermo Fisher (USA). Phosphate buffered saline, Dulbecco's modified Eagle medium (DMEM; high glucose), fetal bovine serum (FBS) and penicillin-streptomycin were purchased from Thermo-Fisher (USA). Protoporphyrin IX(PPIX) was purchased from Sigma Aldrich (USA). Mouse endothelial cell (2H11, ATCC, USA) and mouse pancreatic cancer cells (Panc02) were grown in Dulbecco’s modified Eagle’s medium with high concentrations of glucose (4.5 g/L) and L-glutamine supplemented with 10% fetal bovine serum, penicillin (100 U/mL) and streptomycin (100 µg/mL) (Invitrogen, USA).

2.2 Preparation of PFC droplets and GEM-Lipos. To prepare the PFC droplets, 0.5 ml liquid perfluoro pentane and 4 ml BSA in saline (0.2mg/mL) were mixed and sonicated for 2 min using a bath sonicator (160W, 40 kHz, Bransonic CPX5800, Brandon) until an opaque emulsion can be generated in the water phase. The generated PFC droplets were counted and measured using a microscope (IX81, Olympus, Japan), and analyzed with the ImageJ. Gemcitabine encapsulated liposomes (GEM-Lipo) were prepared by the thin film hydration method as previously

described [23]. Briefly, the mixture of DSPC, DLPC, DSPG, cholesterol, and PPIX was dissolved in a mixed solution of chloroform and methanol (volume ratio 9:1) and then dried in a rotary evaporator (Heidolph G3, Germany) at 40 °C. The prepared thin film was dissolved in *tert*-butanol and followed by freeze-drying. The lipid cake was hydrated with the PBS or gemcitabine solution (50 mg/mL PBS, LC laboratories, USA) by vortexing for 5 minutes. After ten freezing-thawing cycles, the liposome suspension was dialyzed for 48 hours in a dialysis tubing with the molecular cut off of 14,000 kDa to remove unloaded free gemcitabine. The dialysis media (PBS buffer) was changed with fresh media every 8 hours. All the dialysis buffer was collected. The loading content of gemcitabine was calculated from the difference between the initial and left gemcitabine in the dialysis media. The generated GEM-Lipos were imaged using a microscope (IX81, Olympus, Japan), and analyzed with ImageJ. The size distribution of liposomes in PBS was determined through dynamic light scattering (DLS) in a Malvern Zeta-sizer Nano ZS instrument (Malvern Instruments Ltd). The morphology of liposomes was analyzed by scanning electron microscope (SEM, JEOL 5800LV) and transmission electron microscopes (TEM, JEOL 1010).

2.3 Characterization of GEM-Lipo release. A reactive oxygen species (ROS) indicator Carboxy-H_2DCFDA was used to demonstrate ROS generation under acoustic exposure. Immediately prior to use, a fresh stock dye solution was prepared by dissolving Carboxy-H_2DCFDA in ethanol. After PBS dilution, the working solution was added to the liposomes solution to reach a final concentration of 5 μM. The fluorescent emission intensity (emission 493 nm/ excitation 522 nm) was recorded after applying ultrasound to the solution for 3 min. To evaluate the specific acoustically-responsive controlled release of the gemcitabine from the liposomes, the *in vitro* release experiment in the presence of ultrasound was conducted. 300 μL of gemcitabine loaded liposomes were injected in Slide-A-Lyzer Dialysis Cassette (20,000 MWCO, Thermo Fisher, USA). To measure liposomes' response to acoustic treatment, HIFU with different intensity and duration was applied to the sample solution. The gemcitabine concentration in the dialysate was determined using UV-vis spectroscopy at 265 nm. For gemcitabine quantification, samples with different concentrations were measured at the same condition to generate standard curves.

2.4 Characterization of acoustic endothelium disruption. To model the tumor endothelium, 2H11 cells were seeded on the 8 μm-pore- polycarbonate membrane coated with fibronectin to form a monolayer culture. A suspension of 300 μL PFC droplets (concentration 10^9/mL) was added to the transwell. The 2H11 cells on the membrane were treated with different acoustic pressures from 0 to 3 MPa after introducing HIFU to well-plates by coupling a thin layer of ultrasonic transmission gel to a HIFU transducer (H101, Sonic Concept, USA). The transducer was energized by the sinewave radio frequency signal generated by a function generator (AFG3102C, Tektronix, Inc., USA) and amplified by an amplifier (25A100A, Amplifier Research,

USA). Right after, the cells were imaged by a fluorescent microscope (IX83, Olympus, Japan).

2.5 Cell viability test. To test the drug treatment, mouse pancreatic cancer cells (Panc02) were seeded at 1×10^5 cells/well in 96-well plates and pre-incubated for 24 hours before the assay. Then, the medium was replaced with fresh medium containing gemcitabine (10 μM) or medium from the bottom chamber of trans-wells that permeated from top chambers which were treated with HIFU. After 48 hours incubation, the solution of MTT (10 μL) was added to the wells (final concentration 0.5 mg/mL) followed by 4-hour incubation at 37 °C in a humified atmosphere containing 5% CO_2. Finally, the MTT solution was removed and 100 μL of dimethylsulfoxide was added (at 37 °C for 30 minutes) and the absorbance values of the cells per well were determined with a microplate reader (Bio-Tek Epoch, USA) at 570 nm. The background absorbance of the well plate was measured and subtracted. The cell viability was calculated by dividing the optical density values (OD) of the treated groups (T) by the OD of the controls (C) ([T/C ×100%]).

2.6 Animal Study. All experiments were conducted in accordance with the animal guidelines of our institutional animal care and use (IACUC) committee. Female C57BL/6 mice (five-week old, Charles River, IL, USA) were injected with 0.5 million E0771 cells on the mammary fat pad. Tumors were allowed to develop for 13 days until they reach 500-600 mm^3 before acoustic treatment. Animals were anaesthetized and maintained with 2-4% isoflurane on a water heating pad. Ultrasonic gel was applied on the skin around the surface of the tumor. Firstly, 50 μL of 20 mg/mL Evans blue solution (Sigma Aldrich, USA) in saline was injected retro-orbitally, followed by intratumor injection of 50 μL of 50 million microbubbles in 5 minutes. Immediately after the injection of microbubbles, the ultrasound treatment was started and maintained for 5 minutes. 10 minutes after the first injection of microbubbles the second injection was given and the same acoustic treatment was repeated. 65 minutes after the Evans blue injection, the animals were euthanized under CO_2 followed by cervical dislocation. After the mice were euthanized, the skin covering the tumor was removed and photographs were taken, followed by removal of the tumor. The animals were randomized into 4 groups: Blank (without any treatment); Control (Evans blue only); Evans blue, microbubbles, and 2MPa ultrasound treatment; Evans blue, microbubbles, and 4MPa ultrasound treatment. 300 μL of formamide was added to freeze-dried tumor samples. Extraction took place for a minimum of 10 h, during which the sample was left at 60 °C for 2 h, followed by centrifugation at 5000 g for 30 min. Absorption of Evans blue was measured from 100 μL samples at 595 nm. Absorbance was compared with a standard curve of Evans blue in formamide. Evans blue extravasation was calculated as micrograms of Evans blue per milligrams of dry tissue.

3. Results and discussion

3.1 Characterization of PFC droplets and liposomes. Before the co-delivery experiments, we first prepared PFC droplets and liposomes with uniform size and good stability. The PFC droplets were prepared by sonicating liquid perfluoro pentane and BSA in saline. The prepared PFC droplets show a uniform spherical morphology with the average diameter of 1.48 ± 0.49 μm (Fig. 2a). The liposomes were formed by DSPC, DSPG, DLPC, cholesterol and PPIX. The DSPC and DSPG are saturated phospholipids while the DLPC molecule contains four carbon-carbon double bonds which makes the PPIX liposome vulnerable to ROS oxidation. Cholesterol was incorporated to modulate the membrane's fluidity, elasticity, and permeability as a stabilizer by filling the gaps created by imperfect packing of lipids [24]. The prepared liposomes also have a uniform spherical morphology with the average diameter of 1.42 ± 0.40 μm (Fig. 2a). We also tested the liposomes' size variation before and after acoustic treatment. The liposomes with averaged diameter as 1.89 μm decreased about 0.8 μm after acoustic treatment. The size variation before and after acoustic treatment was also confirmed using SEM and TEM images (Fig. 2c and 2d). Before acoustic treatment, the liposomes remained a good stability with minimal release. Less than 12% of Less than 12% of drug were released within 48 hours(Fig. 2e).

3.2 ROS generation. HIFU induced ROS production was measured by a fluorescent indicator Carboxy-H_2DCFDA. Carboxy-H_2DCFDA only becomes fluorescent in the presence of ROS, which oxidizes Carboxy- H_2DCFDA. The fluorescent intensity of liposome with different PPIX ratio was measured under acoustic treatment (Fig. 2f). Increasing of PPIX ratio from 0 to 0.4% led to higher ROS production. The ROS reached the maximum amount when the loading concentration of PPIX was 0.4%. Interestingly, the ROS decreased with further increasing of PPIX concentration (0.8%). This might be because the high concentration PPIX caused self-quenching due to strong π-π stacking and reduced ROS generation[25]. Therefore, PPIX with the concentration of 0.4% was used for the further experiment.

3.3 Acoustically-triggered release. The controlled release is a critical feature for a practical cancer therapy. The anticancer drug, gemcitabine (GEM), was loaded into the aqueous core of liposomes using the thin film hydration method. The loading capacity and encapsulation efficiency of GEM were 8.7% and 24.4% (Fig. 3a), respectively, which matches with previous studies [26]. To evaluate the acoustically-triggered release of GEM from liposomes, the *in vitro* release experiment was conducted. The releasing rate of GEM was obtained from the slope of the linear-fitted curve, and the releasing rate increased as acoustic pressure increasing from 1 MPa to 3 MPa (Fig. 3a). Moreover, the HIFU was applied to the liposome solution in a pulsatile manner (Fig. 3b). Without HIFU, a negligible amount of drug was released over a period of 10 min. In contrast, HIFU dramatically increased GEM release rate to 0.63 ± 0.07%/min. These results indicated an on-off release feature by HIFU.

3.4 Disruption of tumor endothelial cells. Previous studies have shown that HIFU might contribute to the disruption of tumor vasculatures, thus reducing tumor drug resistance [27]. However, this phenomenon has yet been utilized in combination with acoustically-mediated drug release. Therefore, in order to deliver the drug as well as disrupt the blood-tumor barrier simultaneously, we first evaluated the acoustic treatment on endothelial cell monolayer culture. An endothelial cell disruption assay was performed by using an *in vitro* transwell model. Briefly, a monolayer of endothelial cells 2H11 was seeded on the porous polycarbonate membrane with 8 μm pores to form monolayer which mimics the microvasculature in the tumor microenvironment. After the cells reached confluence on the membrane, 200 μL of PFC droplets suspension with a concentration of 1×10^9/mL was added to the upper layer of a transwell insert (Fig. 4a) followed by acoustic treatment for 3 minutes. In the presence of 1 MPa acoustic pressure HIFU had a minimal effect on the integrity of the endothelial monolayer (Fig. 4b). However, HIFU with an acoustic pressure of 2 MPa induced significant perforations (intercellular gaps) within the endothelial monolayer. This observation is supported by results and predictions of previous studies[27][28]. When the acoustic pressure further increased to 3 MPa, the disturbance is so strong that all the cells are detached from the transwell membrane. It is reported that a large peak negative acoustic pressure may be harmful to normal tissue[29]. Based on these results, an acoustic pressure of 2 MPa, and a treatment duration of 3 minutes was chosen for subsequent experiments.

3.5 Synergetic anticancer effect of PFC droplets and GEM-Lipo. After the successful demonstration of acoustic endothelium disruption, we further employed this effect to enhance the efficacy of cancer chemotherapy. To mimic the intratumor delivery of GEM *in vivo*, we set up an experiment where PFC droplets and GEM-Lipo were simultaneously added to the upper chamber of 2H11 confluent transwell as described above (Fig. 4a). Using a monolayer of endothelial cell culture, we expect that PFC droplets can enhance the permeability of endothelium layer. The GEM-Lipo can then be triggered to release GEM into the lower chamber of transwell (Fig. 4a). The culture medium in the lower chamber of the transwell was then collected for the cytotoxicity assay. The collected medium with GEM was applied onto murine pancreatic cancer culture (Panc02) to test the effect of acoustic treatment. Briefly, Panc02 cells were seeded in the 96 well plate at 10,000 cells per well one day before. We treated the Panc02 cells with the medium collected from the lower chamber of the transwell assay and tested their viability using the colorimetric MTT assay. Figure 4c shows the viability of Panc02 cells in 48 hours after treatments with the indicated condition. The dose of gemcitabine (10 μM) in each transwell is determined elsewhere[30]. The cells subjected to PFC droplets and GEM-Lipo upon insonation showed a significant increase in cytotoxicity compared to the control group that receives no treatment. Without PFC droplets the anti-tumor efficacy is weaker

indicating the importance of PFC droplets in the opening of the endothelial monolayer, thus better penetration of the drug into tumor stroma. The viability of cells in the free drug group is low probably due to the diffusion of small drug molecules through the semi-permeable transwell membrane, indicating that free drug can penetrate through the vasculature without specificity. In contrast, the cells subjected to PFC droplets and GEM-Lipo without HIFU showed minimal cytotoxicity compared with the control group with the same drug concentration, suggesting that PFC droplets and GEM-Lipo are stable under normal physiological conditions.

3.6 Testing in animal model. We confirmed that this acoustically-mediated delivery strategy could enhance therapeutic efficacy by enhancing local extravasation and controlled release of anti-cancer drugs in an *in vitro* model. We further conducted *in vivo* experiments in the mouse tumor model with the aim to quantify the enhancement of intratumor delivery in the orthotopic mouse tumor (Fig. 5a). To characterize the disruption of tumor endothelium, we used an albumin binding dye Evans blue. This dye can bind to blood-borne albumin to test blood perfusion in tumor under acoustic treatment [31]. Evans blue is a relevant marker to study enhanced extravasation of small molecule drugs. We retro-orbitally injected Evans blue and conducted intratumor injection with PFC droplets and liposomes to investigate blood perfusion into the orthotopic tumor without acoustic treatment. There might be concerns that these relatively large sized liposomes or carriers may get trapped in the lungs and cause pneumothorax. In the future work, nanoscale delivery carriers will be developed. We found the minimal dye diffusion into the tumor (22.93 μg/mg of tumor), indicating that this dye could not permeate efficiently through blood-tumor barrier alone. In contrast, a 2 MPa acoustic treatment (92.04 μg/mg of tumor) made about 4-fold higher dye tumor diffusion compared with the control group, indicating the disruption of tumor endothelium as well as the enhancement of drug delivery into solid tumors (Fig. 5 b,c). We further evaluated the impact of acoustic pressure on the dye diffusion. There is a trend that the dye tumor diffusion will increase with acoustic pressure. However, there is an enhancement only about 13.65% from 2 MPa to 4 MPa (104.60 μg/mg of tumor @ 4 MPa v.s. 92.04 μg/mg of tumor @ 2MPa). Therefore, we demonstrated the tumor endothelium disruption and improvement of drug delivery *in vivo*.

4. Conclusion

In summary, we developed a new acoustically-mediated delivery method for the improvement of cancer chemotherapy by disrupting tumor endothelium and digitally releasing the cancer chemotherapeutics. We demonstrated that acoustically-oscillating microbubbles could significantly increase the permeability of the endothelium *in vitro*. On this basis, the hybridized liposomes with the sonosensitizer (PPIX) serving as an acoustically-responsive carrier could achieve on-demand delivery of anti-tumor drugs. We also validated this strategy with a tumor xerograph

model successfully and demonstrated the enhancement of drug delivery and disruption of tumor endothelium *in vivo*. In conclusion, we envision this novel syngeneic delivery strategy using liposome carriers and PFC droplets could be adopted by the already widely acoustic treatments in the clinics to limit off-target toxicity as well as enhance drug penetration into tumor stroma.

Acknowledgments

This project was funded by departmental startup funds of Indiana University Bloomington and the Vice Provost for the Research through the Faculty Research Support Program (Indiana University Bloomington).

ORCID iDs

Feng Guo https://orcid.org/0000-0001-9103-3235

References.

[1] Neoptolemos J P, Palmer D H, Ghaneh P, Psarelli E E, Valle J W, Halloran C M, Faluyi O, O'Reilly D A, Cunningham D, Wadsley J, Darby S, Meyer T, Gillmore R, Anthoney A, Lind P, Glimelius B, Falk S, Izbicki J R, Middleton G W, Cummins S, Ross P J, Wasan H, McDonald A, Crosby T, Ma Y T, Patel K, Sherriff D, Soomal R, Borg D, Sothi S, Hammel P, Hackert T, Jackson R and Büchler M W 2017 Comparison of adjuvant gemcitabine and capecitabine with gemcitabine monotherapy in patients with resected pancreatic cancer (ESPAC-4): a multicentre, open-label, randomised, phase 3 trial *Lancet* **389** 1011–24

[2] Conroy T, Desseigne F, Ychou M, Bouché O, Guimbaud R, Bécouarn Y, Adenis A, Raoul J-L, Gourgou-Bourgade S, de la Fouchardière C, Bennouna J, Bachet J-B, Khemissa-Akouz F, Péré-Vergé D, Delbaldo C, Assenat E, Chauffert B, Michel P, Montoto-Grillot C and Ducreux M 2011 FOLFIRINOX versus Gemcitabine for Metastatic Pancreatic Cancer *N. Engl. J. Med.* **364** 1817–25

[3] Siegel R L, Miller K D and Jemal A 2018 Cancer statistics, 2018 *CA. Cancer J. Clin.* **68** 7–30

[4] Von Hoff D D, Ervin T, Arena F P, Chiorean E G, Infante J, Moore M, Seay T, Tjulandin S A, Ma W W, Saleh M N, Harris M, Reni M, Dowden S, Laheru D, Bahary N, Ramanathan R K, Tabernero J, Hidalgo M, Goldstein D, Van Cutsem E, Wei X, Iglesias J and Renschler M F 2013 Increased Survival in Pancreatic Cancer with nab-Paclitaxel plus Gemcitabine *N. Engl. J. Med.* **369** 1691–703

[5] Dubey R D, Saneja A, Gupta P N P K and Gupta P N P K 2016 Recent advances in drug delivery strategies for improved therapeutic efficacy of gemcitabine *Eur. J. Pharm. Sci.* **93** 147–62

[6] Arumugam T, Ramachandran V, Fournier K F, Wang H, Marquis L, Abbruzzese J L, Gallick G E, Logsdon C D, McConkey D J and Choi W 2009 Epithelial to Mesenchymal Transition Contributes to Drug Resistance in Pancreatic Cancer *Cancer Res.* **69** 5820–8

[7] Mitra S, Sasmal H S, Kundu T, Kandambeth S, Illath K, Díaz Díaz D and Banerjee R 2017 Targeted Drug Delivery in Covalent Organic Nanosheets (CONs) via Sequential Postsynthetic Modification *J. Am. Chem. Soc.* **139** 4513–20

[8] Guo X, Shi C, Wang J, Di S and Zhou S 2013 pH-triggered intracellular release from actively targeting polymer micelles *Biomaterials* **34** 4544–54

[9] Obata Y, Tajima S and Takeoka S 2010 Evaluation of pH-responsive liposomes containing amino acid-based zwitterionic lipids for improving intracellular drug delivery in vitro and in vivo *J. Control. Release* **142** 267–76

[10] Perrino E, Steiner M, Krall N, Bernardes G J L, Pretto F, Casi G and Neri D 2014 Curative Properties of Noninternalizing Antibody-Drug Conjugates Based on Maytansinoids *Cancer Res.* **74** 2569–78

[11] Xu J-H, Gao F-P, Li L-L, Ma H L, Fan Y-S, Liu W, Guo S-S, Zhao X-Z and Wang H 2013 Gelatin–mesoporous silica nanoparticles as matrix metalloproteinases-degradable drug delivery systems in vivo *Microporous Mesoporous Mater.* **182** 165–72

[12] Kim H, Kim S, Park C, Lee H, Park H J and Kim C 2010 Glutathione-induced intracellular release of guests from mesoporous silica nanocontainers with cyclodextrin gatekeepers *Adv.*

Mater. **22** 4280–3

[13] Chen K J, Liang H F, Chen H L, Wang Y, Cheng P Y, Liu H L, Xia Y and Sung H W 2013 A thermoresponsive bubble-generating liposomal system for triggering localized extracellular drug delivery *ACS Nano* **7** 438–46

[14] Yuan Q, Zhang Y, Chen T, Lu D, Zhao Z, Zhang X, Li Z, Yan C H and Tan W 2012 Photon-manipulated drug release from a mesoporous nanocontainer controlled by azobenzene-modified nucleic acid *ACS Nano* **6** 6337–44

[15] Mura S, Nicolas J and Couvreur P 2013 Stimuli-responsive nanocarriers for drug delivery *Nat. Mater.* **12** 991–1003

[16] Sirsi S R and Borden M A 2014 State-of-the-art materials for ultrasound-triggered drug delivery *Adv. Drug Deliv. Rev.* **72** 3–14

[17] Aryal M, Arvanitis C D, Alexander P M and McDannold N 2014 Ultrasound-mediated blood-brain barrier disruption for targeted drug delivery in the central nervous system *Adv. Drug Deliv. Rev.* **72** 94–109

[18] Wood A K W and Sehgal C M 2015 A review of low-intensity ultrasound for cancer therapy *Ultrasound Med. Biol.* **41** 905–28

[19] Furusawa Y, Fujiwara Y, Hassan M A, Tabuchi Y, Morita A, Enomoto A and Kondo T 2012 Inhibition of DNA-dependent protein kinase promotes ultrasound-induced cell death including apoptosis in human leukemia cells *Cancer Lett.* **322** 107–12

[20] Furusawa Y, Fujiwara Y, Campbell P, Zhao Q-L, Ogawa R, Ali Hassan M, Tabuchi Y, Takasaki I, Takahashi A and Kondo T 2012 DNA Double-Strand Breaks Induced by Cavitational Mechanical Effects of Ultrasound in Cancer Cell Lines ed M G Marinus *PLoS One* **7** e29012

[21] Pinton G, Aubry J-F, Bossy E, Muller M, Pernot M and Tanter M 2011 Attenuation, scattering, and absorption of ultrasound in the skull bone *Med. Phys.* **39** 299–307

[22] Hynynen K, Clement G, McDannold N, Vykhodtseva N, White P J, Jolesz F A and Sheikov N A 2004 The feasibility of noninvasive image-guided treatments of brain disorders by focused ultrasound *J. Acoust. Soc. Am.* **115** 2446–7

[23] Rwei A Y, Paris J L, Wang B, Wang W, Axon C D, Vallet-Regí M, Langer R and Kohane D S 2017 Ultrasound-triggered local anaesthesia *Nat. Biomed. Eng.* **1** 644–53

[24] Briuglia M-L, Rotella C, McFarlane A and Lamprou D A 2015 Influence of cholesterol on liposome stability and on in vitro drug release *Drug Deliv. Transl. Res.* **5** 231–42

[25] Jia H-R, Jiang Y-W, Zhu Y-X, Li Y-H, Wang H-Y, Han X, Yu Z-W, Gu N, Liu P, Chen Z and Wu F-G 2017 Plasma membrane activatable polymeric nanotheranostics with self-enhanced light-triggered photosensitizer cellular influx for photodynamic cancer therapy *J. Control. Release* **255** 231–41

[26] Cosco D, Federico, Morittu, Britti and Trapasso 2012 Gemcitabine-loaded liposomes: rationale, potentialities and future perspectives *Int. J. Nanomedicine* 5423

[27] Caskey C F, Stieger S M, Qin S, Dayton P A and Ferrara K W 2007 Direct observations of ultrasound microbubble contrast agent interaction with the microvessel wall *J. Acoust. Soc. Am.* **122** 1191–200

[28] Prentice P, Cuschieri A, Dholakia K, Prausnitz M and Campbell P 2005 Membrane disruption by optically controlled microbubble cavitation *Nat. Phys.* **1** 107–10

[29] Zhang M, Fabiilli M L, Haworth K J, Fowlkes J B, Kripfgans O D, Roberts W W, Ives K A and Carson P L 2010 Initial investigation of acoustic droplet vaporization for occlusion in canine kidney. *Ultrasound Med. Biol.* **36** 1691–703

[30] Torres M P, Rachagani S, Souchek J J, Mallya K, Johansson S L and Batra S K 2013 Novel Pancreatic Cancer Cell Lines Derived from Genetically Engineered Mouse Models of Spontaneous Pancreatic Adenocarcinoma: Applications in Diagnosis and Therapy ed F H Sarkar *PLoS One* **8** e80580

[31] Bekeredjian R, Kroll R D, Fein E, Tinkov S, Coester C, Winter G, Katus H A and Kulaksiz H 2007 Ultrasound Targeted Microbubble Destruction Increases Capillary Permeability in Hepatomas *Ultrasound Med. Biol.* **33** 1592–8

Figures and captions

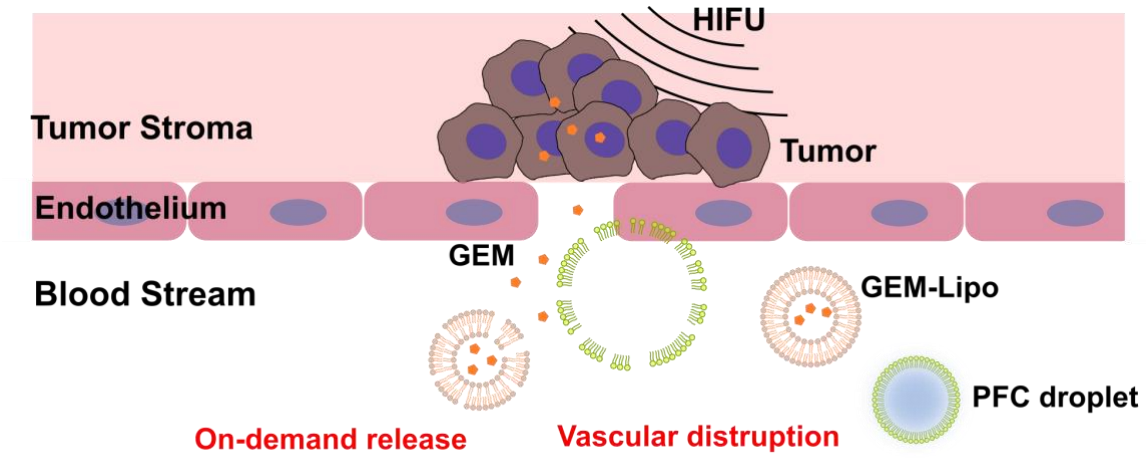

Figure 1. Schematic representation of the proposed acoustically-responsive release of drugs and enhanced extravasation in the tumor microenvironment.

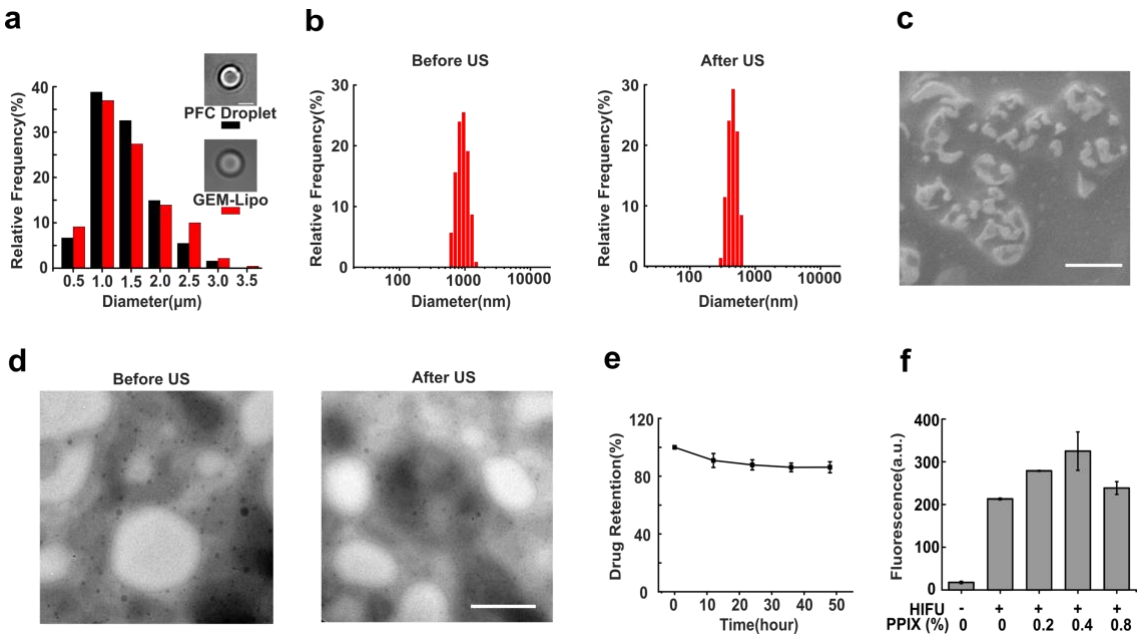

Figure 2. (a) Size distribution and morphology (insets) of PFC droplets and GEM-Lipo liposomes. b) Size distribution of liposomes before and after acoustic treatment. c) SEM image of liposomes. d) TEM images of liposomes before and after acoustic treatment. e) Drug retention in liposomes over a period of 48 hours. (f) Reactive oxygen species (ROS) generation by PPIX loading in the GEM-Lipo measured by a fluorescent indicator. Scale bar: 2 μm.

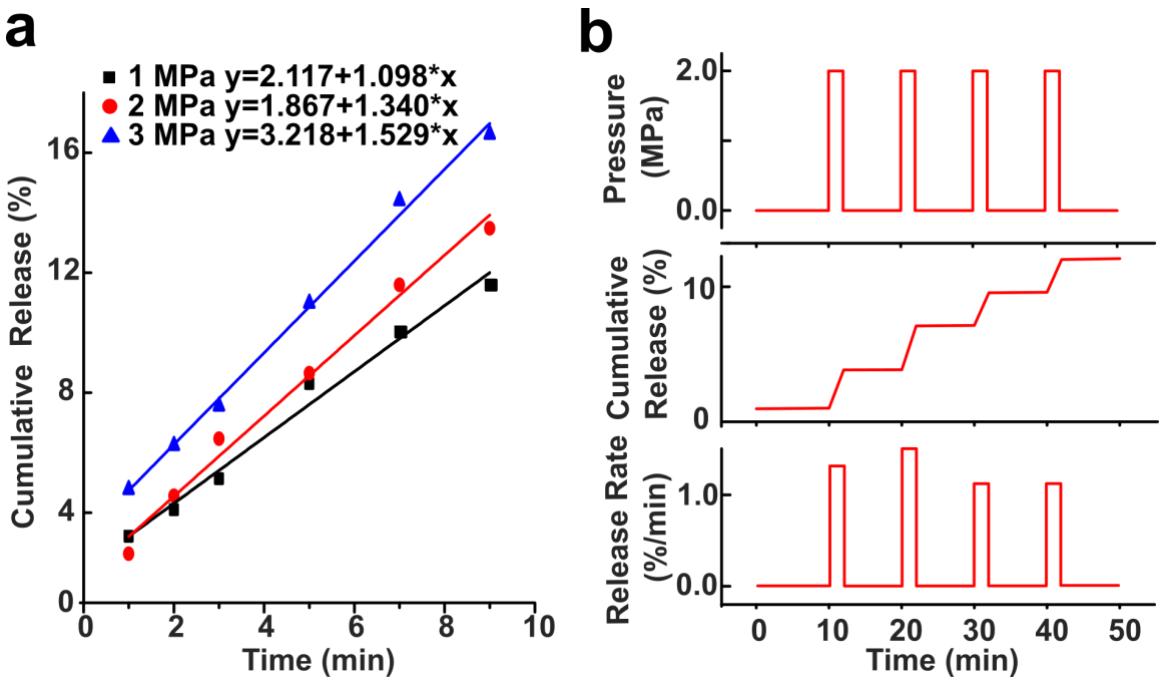

Figure 3. (a) *In vitro* drug release as a function of HIFU duration and acoustic pressure. **(b)** The on-off effect of HIFU on drug release from GEM-Lipo (for 2 min, applied once every 10 min). The digital regulation of acoustic pressures (up), the cumulative release (middle) and release rate (bottom) of drug (GEM).

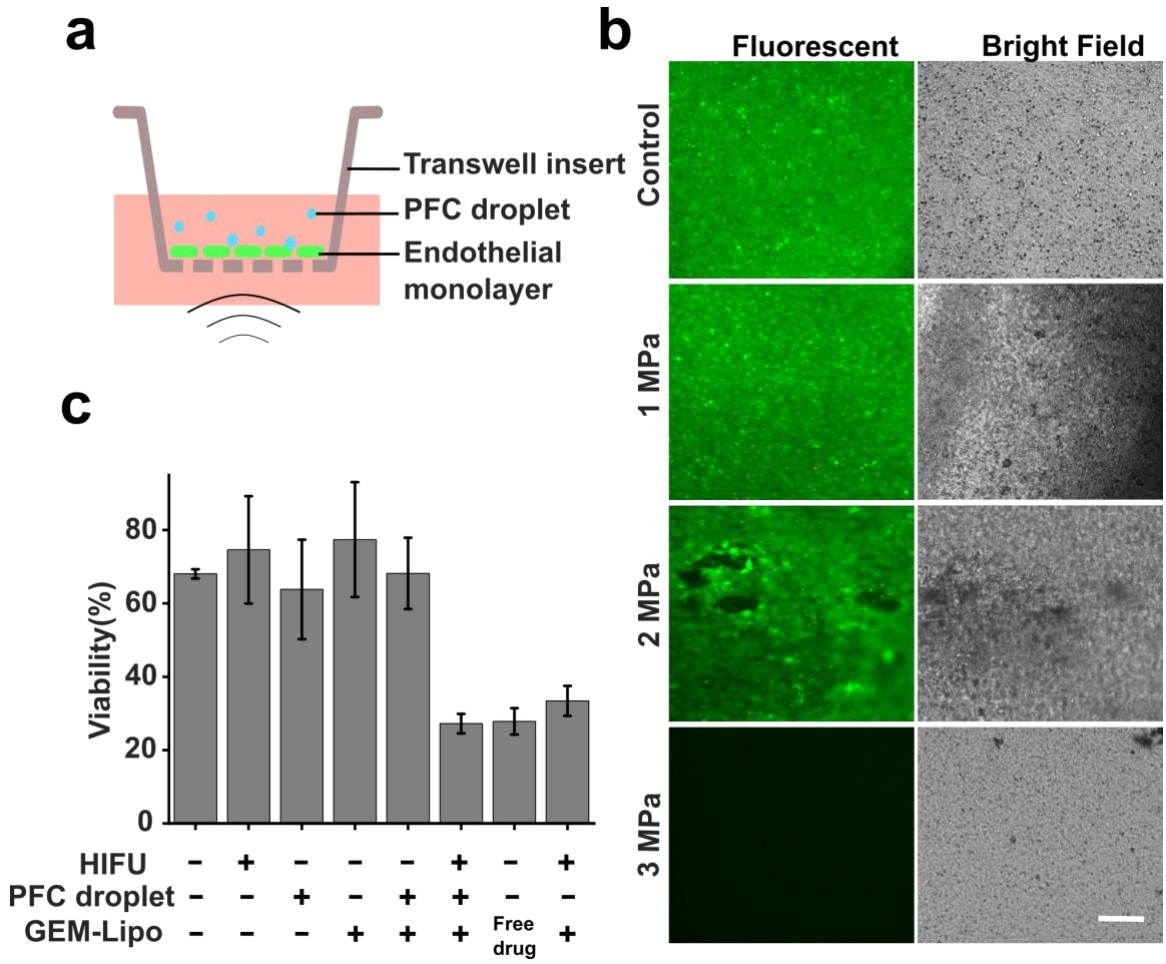

Figure 4. (a) Schematic of the experimental setup for the *in vitro* endothelial monolayer with HIFU. **(b)** Fluorescent staining of endothelial cells treated with different acoustic pressure for 3 minutes. **(c)** Cell viability of Panc02 after 48 hours under different treatments. Scale bar: 100 μm

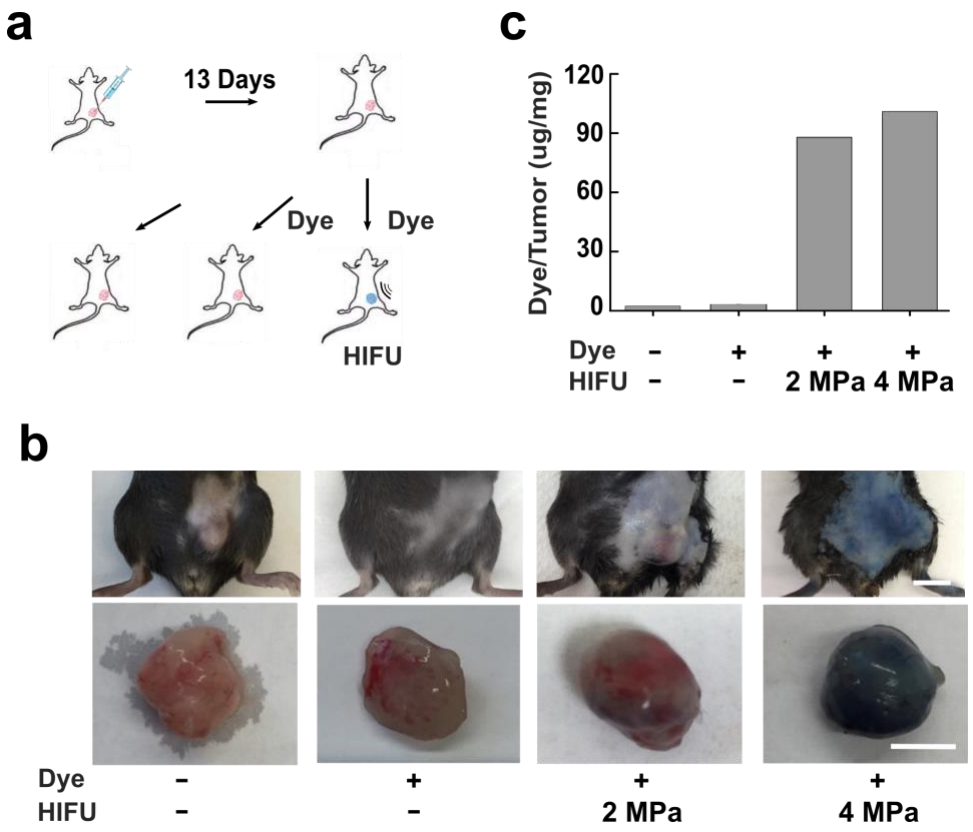

Figure 5. (a) Experimental design of *in vivo* study. **(b)** Images of dye (Evans blue) penetration into tumors of living mice under different acoustic treatments (0, 2, and 4 MPa). **(c)** The quantitation of dye (Evans blue) penetration into tumor tissues. Scale bar: 500 µm